Droplet State and the Compressibility Anomaly in Dilute 2D Electron Systems

Junren Shi[1] and X. C. Xie[1,2]

[1]*Department of Physics, Oklahoma State University, Stillwater, Oklahoma 74078*
[2]*International Center for Quantum Structures and Institute of Physics, Chinese Academy of Sciences, Beijing, China*
(Received 22 March 2001; published 6 February 2002)

We investigate the space distribution of carrier density and the compressibility of two-dimensional (2D) electron systems by using the local density approximation. The strong correlation is simulated by the local exchange and correlation energies. A slowly varied disorder potential is applied to simulate the disorder effect. We show that the compressibility anomaly observed in 2D systems which accompanies the metal-insulator transition can be attributed to the formation of the droplet state due to a disorder effect at low carrier densities.

The recent discovery [1] of a two-dimensional (2D) metal-insulator transition (MIT) has raised the important question concerning the existence of a metallic phase in 2D systems. In contrast to the scaling theory of localization [2], which predicts that only an insulating phase exists in 2D, there is strong experimental evidence [1] for metallic-like behavior in many 2D samples. This should not be totally surprising because the dominant Coulomb interaction in these systems may invalidate the noninteracting scaling theory. These intriguing experiments generate renewed interest in studying the properties of low-density 2D electron systems, especially in the combined effects of interaction and disorder in such systems [1]. Most experimental work in the past has concentrated on transport measurements. Some recent experimental studies [3,4] on thermodynamic properties, such as compressibility κ in 2D systems, have shed further light on understanding the 2D MIT. It is found [3] that the negative $1/\kappa$ at low densities reaches a minimum value at a certain density n, and then increases dramatically with further decreasing n. Although this surprising upturn of $1/\kappa$ (compressibility anomaly) was observed much earlier in a pioneering work by Eisenstein *et al.* [5], this is the first time that the minimum point in $1/\kappa$ is identified as the critical density for the 2D MIT [3]. On the theory side, there are recent efforts [6,7] in addressing the interplay between interaction and disorder, and their effect in thermodynamic properties.

In this Letter, we investigate the space distribution of carrier density and the compressibility of 2D electron systems by using the local density approximation. The strong correlation in such systems is simulated by the local exchange and correlation energies. A slowly varied disorder potential is applied to simulate the disorder effect. We find that at low average densities electrons form a droplet state which is a coexistence phase of high- and low-density regions. We show that the compressibility anomaly observed in 2D systems that accompanies the metal-insulator transition can be attributed to the formation of the droplet state [8]. The phase separation has been seen in a recent experiment [9].

To investigate the density distribution of a disordered 2D electron system, we use the density functional theory. The total energy functional reads

$$E[\mathbf{n}] = E_T[\mathbf{n}] + E_{ee}[\mathbf{n}] + E_d[\mathbf{n}] + E_x[\mathbf{n}] + E_c[\mathbf{n}].$$

Here $E_T[\mathbf{n}]$ is the functional of the kinetic energy, $E_{ee}[\mathbf{n}]$ is the direct Coulomb energy due to the charge inhomogeneity, and $E_d(\mathbf{n})$ is the potential energy due to the disorder. The strong correlation effect caused by the electron-electron interaction is included in the final two terms: $E_x[\mathbf{n}]$ is the exchange energy and $E_c[\mathbf{n}]$ is the correlation energy. The ground state density distribution can be obtained by minimizing the total energy functional with respect to the density.

Using the local density approximation, the total exchange and correlation energies are written as

$$E_{x(c)}[\mathbf{n}] \approx \int d\mathbf{x}\, \epsilon_{x(c)}^0[\mathbf{n}(\mathbf{x})]\mathbf{n}(\mathbf{x}),$$

where $\epsilon_{x(c)}^0(n)$ is the exchange (correlation) energy density for a homogeneous 2D electron system at a given density n, which can be determined by quantum Monte Carlo calculations. In this paper, we use the result from Tanatar and Ceperley [10],

$$\epsilon_x^0(n) = -\frac{8}{3}\sqrt{\frac{2}{\pi}}\sqrt{n},$$

$$\epsilon_c^0(n) = a_0 \frac{1 + a_1 x}{1 + a_1 x + a_2 x^2 + a_3 x^3},$$

where $x = 1/(\pi n)^{1/4}$. The energy unit is 1 Ry $= me^4/2\varepsilon^2\hbar^2$, with ε being the dielectric constant and m the effective mass of an electron. The values for the parameters are $a_0 = -0.3568$, $a_1 = 1.13$, $a_2 = 0.9052$, and $a_3 = 0.4165$.

The kinetic energy functional can be written as

$$E_T[\mathbf{n}] = \int d\mathbf{x} \sum_{s,i} \psi_{is}^\dagger(\mathbf{x})(-\nabla^2)\psi_{is}(\mathbf{x}),$$

where the sum is over all occupied quasiparticle energy levels (i) and the spin index (s).

The energy functional for the disorder potential $V_d(\mathbf{x})$ can be written as

$$E_d[\mathbf{n}] = \int d\mathbf{x}\, V_d(\mathbf{x})\mathbf{n}(\mathbf{x}).$$

Two kinds of disorder potentials are used in this work.

(i) The off-plane charge impurity potential:

$$V_d(\mathbf{x}) = -\sum_i \frac{1}{\sqrt{|\mathbf{x} - \mathbf{x}_i|^2 + d^2}},$$

where d is the distance between the electron and the impurity planes, and the impurities are randomly distributed with a density n_i.

(ii) The correlated disorder potential with the correlation between the different positions:

$$\langle V_d(\mathbf{x})V_d(\mathbf{x}')\rangle = V_s^2 \exp\left(-\frac{|\mathbf{x} - \mathbf{x}'|}{\xi}\right),$$

where V_s is the amplitude of the potential fluctuation, and ξ is the correlation length of the disorder. The model simulates a slowly varied disorder potential, and ξ is roughly the average size of valleys in a disorder landscape.

The density distribution of the ground state can be obtained by minimizing the energy functional under the constraint of a constant total electron number. One gets the effective single particle Schödinger equation,

$$[-\nabla^2 + V_{\text{sc}}[\mathbf{n}, \mathbf{x}]]\psi_{is}(\mathbf{x}) = \epsilon_{is}\psi_{is}(\mathbf{x}), \quad (1)$$

where

$$V_{\text{sc}}[\mathbf{n}, \mathbf{x}] = V_d(\mathbf{x}) + \frac{\delta}{\delta\mathbf{n}}[\epsilon_x^0[\mathbf{n}]\mathbf{n} + \epsilon_c^0[\mathbf{n}]\mathbf{n}]$$

is the potential self-consistently determined by the density distribution. $\mathbf{n}(\mathbf{x}) = \sum_{is}|\psi_{is}(\mathbf{x})|^2$, where the sum is over all occupied quasiparticle energy levels and the spin index.

To further simplify the calculation, we make an approximation to the kinetic energy so that it can be written in the form of a density functional [11]:

$$E_T[\mathbf{n}] \approx \int d\mathbf{x}\left[\pi\mathbf{n}(\mathbf{x})^2 + \frac{1}{4}\frac{|\nabla\mathbf{n}(\mathbf{x})|^2}{\mathbf{n}}(\mathbf{x}) + \cdots\right]. \quad (2)$$

The first term provides the local density approximation for the kinetic energy, while the second term includes the effect of the density gradient.

To minimize the total energy functional with the constraint of a constant total electron number, we introduce the new variable χ so that

$$\mathbf{n}(\mathbf{x}) \equiv N\frac{\chi(\mathbf{x})^2}{\int d\mathbf{x}'\,\chi(\mathbf{x}')^2},$$

where N is the total number of the electrons in the system. The constraint for the constant total electron number is automatically satisfied with the new variable. The steepest descent method [11] is used to minimize the total energy functional to χ,

$$\chi^{m+1}(\mathbf{x}) = \chi^m(\mathbf{x}) - \gamma\frac{\delta E[\chi]}{\delta\chi}\bigg|_{\chi=\chi^m(\mathbf{x})},$$

where γ is the iteration constant which is chosen so that the interaction is convergent, and the chemical potential can be calculated by

$$\mu = \frac{\int d\mathbf{x}\,\chi(\mathbf{x})[-\nabla^2 + 2\pi\mathbf{n} + V_{\text{sc}}[\mathbf{n}, \mathbf{x}]]\chi(\mathbf{x})}{\int d\mathbf{x}\,\chi(\mathbf{x})^2}.$$

The calculation is carried out in a 128×128 discrete space. The size of the system is set as $L = 256a_B^*$, where a_B^* is the effective Bohr's radius, $a_B^* = \varepsilon\hbar^2/me^2$. The periodic boundary condition and the Ewald sum for the Coulomb interaction are applied to minimize the finite size effect. The electron density is adjusted by changing the total electron number N. The density distribution is calculated by using the wave function method, [Eq. (1)], and the chemical potential is calculated by using the gradient approximation, [Eq. (2)], which is found to be accurate in calculating the chemical potential comparing to the results obtained from the wave function method.

The compressibility of the system is calculated by

$$\frac{1}{\kappa} = \frac{N^2}{S}\frac{\partial\mu}{\partial N},$$

where S is the total area of the system.

Figure 1 shows the density distribution of the system. It can be clearly seen that the electrons form some high-density regions, while the density of other regions are essentially zero. The boundary of each high-density region can be easily identified because the density rapidly decays to zero beyond the boundary. The electron number contained in each high-density region depends on the detail landscape of the disorder. For the specific disorder potential used in the calculation, there are 3–10 electrons in each high-density region. Depending on the average density of the system, the high-density regions may connect to each other ($r_s = 10$), or form some isolated regions ($r_s = 19$). There exists a certain density ($r_s = 14$), where the high-density regions start to percolate through the system, and form a conducting channel. The calculation clearly demonstrates the idea of our earlier theory [8], i.e., the metal-insulator transition observed in the 2D electron systems is the percolation transition of the electron density.

The electron-electron interaction is important for the conducting behavior of a dilute electron system in the sense that it makes the density distribution more extended because of the Coulomb repulsion. Figure 2 shows the density distribution for the free electron gas with the same density as in Fig. 1(b) by turning off the electron-electron interaction. The system forms only some isolated high-density regions at the disorder valleys, while the density distribution of the corresponding interacting system [Fig. 1(b)] is quite extensive at the same density. At a given disorder strength, the critical density for the free electron gas is much higher than its interacting counterpart.
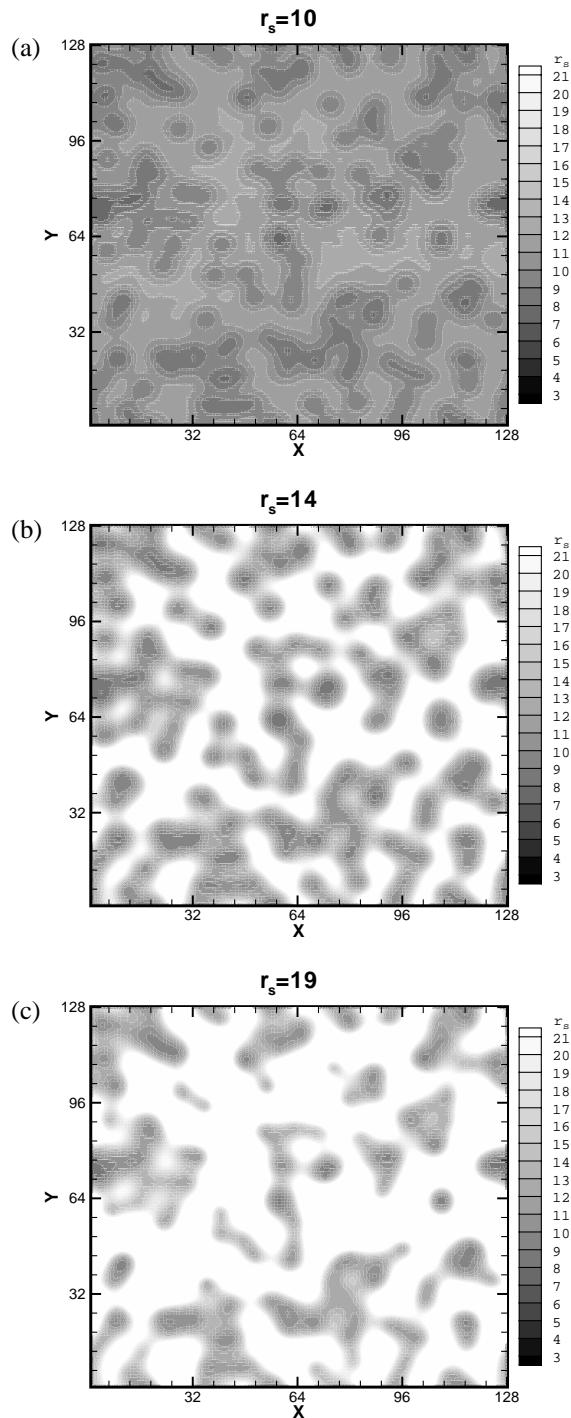
(a) r_s=10

(b) r_s=14

(c) r_s=19

FIG. 1. The density distributions for the different electron densities. We use the contour plot for the local density parameter $r_s = 1/\sqrt{\pi n}$. The density of the white area decreases rapidly to zero. The disorder potential is generated by off-plane charge impurities with $d = 10a_B^*$, $n_i = 2.5 \times 10^{-3}/a_B^{*2}$.

FIG. 2. The density distribution for the free electron gas on the same disorder landscape as Fig. 1 at density $r_s = 14$.

Figure 3 shows the compressibility of the systems. To compare with the experiments [3,5], we calculate $\delta\mu/\delta N$, which is the direct measured quantity in the experiments. It is well known that the compressibility of a uniform electron gas is negative in the low-density region due to the ef-
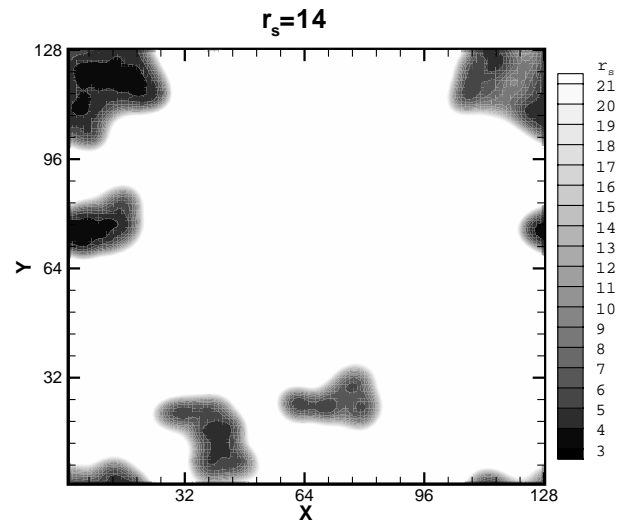
fect of the exchange and correlation energies, as shown by the solid line in Fig. 3(a). However, when the disorder is present, the behavior changes greatly. In the low density, the electrons tend to occupy the valleys of the disorder landscape, and the local density, instead of the average density, determines the compressibility of the system. On the other hand, at higher densities, all of the valleys are filled, and one can expect the compressibility of the system to resume the behavior of a uniform electron gas. We have a nonmonotonic behavior for $\delta\mu/\delta N$, as shown by the squares in Fig. 3(a), which are in good agreement with the experimental measurement [3,5]. Comparing with Fig. 1, we find that the turning point of the compressibility ($N \approx 100$, $r_s \approx 14$) coincides with the percolation threshold of the system. At low densities, the data points in the plot show strong fluctuation, indicating the effect of the local fluctuation of the disorder potential.

The compressibility anomaly is caused by the inhomogeneity of spatial distribution of the electrons. In this case, local density, instead of average density, determines the total energy of the system. Following the definition of the chemical potential, we have

$$\mu(N) \approx \frac{\delta}{\delta N}\{\varepsilon_0[n_{\text{eff}}(N)]N\},$$

where $\varepsilon_0(n)$ is the energy per electron for the uniform electron gas, and n_{eff} is the effective local density. The effective local density can be estimated by $n_{\text{eff}}(n) \approx n/f(n)$, where $f(n)$ is the fraction of the high-density region. In the low-density limit, $f(n) \to 0$. As a consequence, the density dependence of the chemical potential, $\delta\mu/\delta n$, changes greatly. In general, supposing $f(n) \sim n^\alpha$ in the low-density limit, the analysis shows that $\delta\mu/\delta n$ will have a nonmonotonic behavior if $\alpha > 1$. The behavior of $f(n)$ is determined by the local disorder potential profile. In a 2D system, the infinite harmonic potential has $f(n) \sim n$.
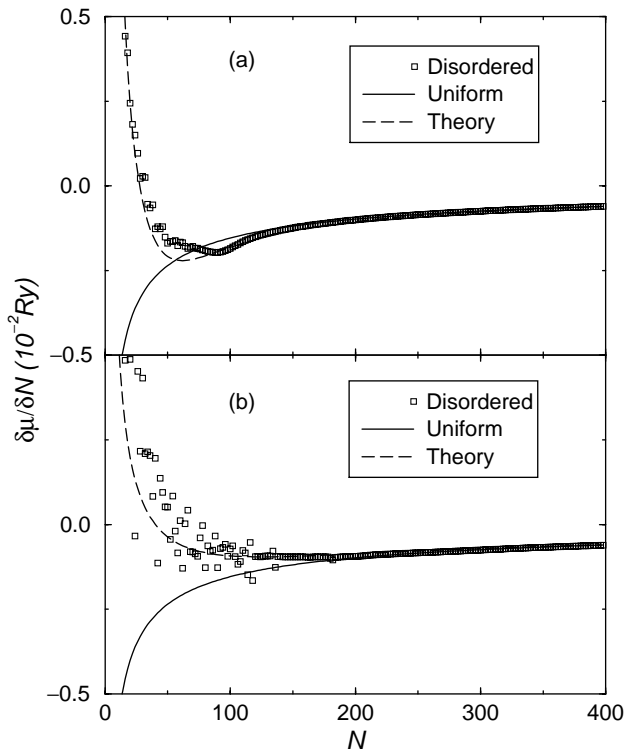
FIG. 3. $\delta\mu/\delta N$ as a function of the electron density. Solid lines are for the uniform electron gas, squares are the data points for the disordered system, and the dashed lines are the results from the theory discussed in the text. Two kinds of disorder are used in the calculation: (a) the off-plane charge impurities (the same parameters as in Fig. 1 are used); (b) the correlated disorder potential with $V_s = 0.2$ Ry, $\xi = 0.2L$. The parameters in the dashed lines: (a) $n_0 = 0.5 \times 10^{-3}/a_B^{*2}$, $\alpha = 2.3$; (b) $n_0 = 10^{-3}/a_B^{*2}$, $\alpha = 1.5$. N is the total number of electrons in the simulation box. $N = 60$ corresponds to $r_s = 19$; $N = 100$ corresponds to $r_s = 14$; $N = 200$ corresponds to $r_s = 10$.

So the requirement $\alpha > 1$ is equivalent to the condition that the local disorder potential has a weaker confinement effect than the harmonic potential. In Fig. 3, we use the previous equation for μ with the following relation of $f(n)$ to fit the data:

$$f(n) = \frac{1}{1 + (\frac{n_0}{n})^\alpha} \; .$$

The effect of the detail potential profile can be seen from Fig. 3. The behavior of the compressibility near the turning point shows a great difference in the two kinds of disorder potentials.

Before summarizing, we would like to make some comments. (i) In this paper, we focus on the relation between the spatial distribution of electrons and the compressibility anomaly. The transport properties could be understood with the percolation picture by assuming that the system has a contrast in local conductivities between high- and low-density regions [8]. One problem with the percolation approach is that if the system is quantum in nature

there should not be a 2D quantum percolation. We believe that percolation transition here is semiclassical in nature [8]. (ii) Quantum Monte Carlo calculations [12] claim that there is a phase transition from an unpolarized to a fully polarized state shortly before the transition to a Wigner crystal. If this is the case, it is reasonable to assume that the high-density region is spin unpolarized while the low-density region is spin polarized in GaAs since the GaAs samples have extremely low critical densities. On the other hand, the disorder may play a more essential role in Si samples since their critical densities are much higher. (iii) In our understanding, the compressibility anomaly is caused by disorder and strong interactions. Some of the 2D MIT models in which the disorder effect is not emphasized might have difficulty in addressing the compressibility anomaly.

In conclusion, we have studied the electron space distribution and the compressibility of disordered dilute 2D electron systems by using the local density approximation. Electron distribution confirms the formation of the droplet state that consists of high- and low-density regions. Our calculated compressibility is in good agreement with the experimentally observed behavior showing unexpected anomaly at low densities. The turning point of the compressibility happens around the percolation threshold. Our theory based on the droplet state provides a possible mechanism of the compressibility anomaly.

[1] For a review, see E. Abrahams, S. V. Kravchenko, and M. P. Sarachik, Rev. Mod. Phys. **73**, 251 (2001), and references therein.

[2] E. Abrahams *et al.*, Phys. Rev. Lett. **42**, 673 (1979).

[3] C. Dultz and H. W. Jiang, Phys. Rev. Lett. **84**, 4689 (2000).

[4] S. Ilani, A. Yacoby, D. Mahalu, and H. Shtrikman, Phys. Rev. Lett. **84**, 3133 (2000).

[5] J. P. Eisenstein, L. N. Pfeiffer, and K. W. West, Phys. Rev. Lett. **68**, 674 (1992); J. P. Eisenstein, L. N. Pfeiffer, and K. W. West, Phys. Rev. B **50**, 1760 (1994).

[6] Q. Si and C. M. Varma, Phys. Rev. Lett. **81**, 4951 (1998).

[7] A. A. Pastor and V. Dobrosavljevic, Phys. Rev. Lett. **83**, 4642 (1999).

[8] S. He and X. C. Xie, Phys. Rev. Lett. **80**, 3324 (1998); J. Shi, S. He, and X. C. Xie, Phys. Rev. B **60**, R13 950 (1999); J. Shi and X. C. Xie, Phys. Rev. B **63**, 045123 (2001); J. Shi, S. He, and X. C. Xie, cond-mat/9904393.

[9] S. Ilani, A. Yachoby, D. Mahalu, and H. Shtrikman, Science **292**, 1354 (2001).

[10] B. Tanatar and D. M. Ceperley, Phys. Rev. B **39**, 5005 (1989); S. T. Chui and B. Tanatar, Phys. Rev. Lett. **74**, 458 (1995).

[11] Y. Wang, J. Wang, H. Guo, and E. Zarembar, Phys. Rev. B **52**, 2738 (1995), and references therein.

[12] C. Attaccalite *et al.*, cond-mat/0109492, and references therein.